

Sorption Paper Title

Jonathan G. V. Ström^a, Shuai Xie^a, Eric M. Suuberg^a

These authors contributed equally to this work

^a*Brown University, School of Engineering, Providence, RI, USA*

Abstract

Abstract here

Keywords: Vapor intrusion, Temporal variability, Sorption, Attenuation factor

1. Introduction

Many vapor intrusion (VI) contaminants has the capacity to sorb onto soil and various common indoor materials, but the role and more importantly - the consequences of these sorption processes in VI are poorly understood[1, 2?]. The migration of contaminant vapors from its source into the affected building and potential indoor sources are usually the prime concern in VI investigations. Rarely is the sorbed contaminant vapors in the soil or indoor considered in an investigation, but these may potentially act as a capacitor, storing and releasing contaminant vapors in response to a change in contaminant concentration. Consequently, contaminant vapors may be much more persistent at a site that has undergone remediation, potentially reducing the effectiveness of mitigation systems, or impeding site investigations.

It was well recognized that building materials had capacities to adsorb pollutants. Xu et al. studied the capacity of formaldehyde conventional gypsum wallboard, "green gypsum wall board, and "green" carpets[?]. However, most studies conducted before were at relative high concentration of VOCs, usually mg/m³ or even higher concentration, which is several magnitudes higher than the concentration of VOCs in indoor environment.

Although it is recognized that sorption may be used to treat indoor air contaminants, and passive sorption tube samplers are used prolifically in VI investigations, measuring contaminant sorption onto materials or soils is

Email address: eric_suuberg@brown.edu (Eric M. Suuberg)

29 not a regular part of VI investigations and thus very little is known of the
30 potential impact of this[3].

31 Over the years many VI sites have been investigated for their potential
32 exposure risk. Most of these are conducted by private industries but a few
33 notable academic ventures exist as well. Two well-known examples of these
34 are the studies of "Sun Devil Manor" near Hill Air Force Base in Utah, and
35 a building in Indianapolis, Indiana. Both of these sites were outfitted with a
36 wide variety of instrumentation to investigate the VI drivers at these sites.
37 These studies yielded some of the richest VI datasets available and gave
38 invaluable insights, in particular in the application of CPM[4] and sub-slab
39 depressurization (SSD) mitigation systems[5, 6]. However, neither of these
40 studies considered the role of sorption had at these sites.

41 The potential impact of sorption may perhaps be most significant in the
42 application of the controlled pressure method and various mitigation schemes.
43 The controlled pressure method (CPM) is the forced over- and depressur-
44 ization of a building to max- and minimize the contaminant entry to the
45 building. This aids the investigator to ascertain the worst-case VI scenario
46 and help identify potential indoor contaminant sources[7, 4]. However, if
47 the building has a large capacity to sorb contaminant vapors onto various
48 materials, these may be sorbed and desorbed in response to the changing
49 condition, potentially preventing corresponding changes in indoor air con-
50 taminant concentrations. The same is true for various mitigation schemes,
51 while they may successfully prevent contaminant vapors from entering the
52 house, these may still be released from the interior over an unknown period
53 of time[1, 2].

54 In the past VI models have been used to gain insight into VI when no field
55 or experimental data has been available. Previously examples of VI modeling
56 studies are the role of rainfall in VI[8], or drivers of temporal variability in
57 some of the aforementioned sites[9]. However, while many VI models include
58 a sorption term in the governing equation for contaminant transport in soils,
59 none have explored the role of sorption in VI. The reason for this is two-fold.
60 First, there has been a general lack of interest in sorption and VI thus far.
61 Secondly, the vast majority of VI modeling efforts and studies has focused
62 on steady-state analyses of VI, and sorption only affects soil contaminant
63 transport in time-dependent scenarios.

64 To bridge this knowledge gap we will begin to explore the role of sorp-
65 tion in VI through a combined effort of experimental and simulation work.
66 Sorption data of TCE on various common indoor materials and Appalian

soil will be measured in a flow-chamber experiment. These sorption data will then be incorporated into a three-dimensional finite element model of VI. For this purpose we will consider a prototypical VI scenario where a free-standing house with a basement is overlying a homogenously contaminated groundwater source. Using this model we will investigate how the dynamic contaminant transport is affected in general by sorption, how indoor sorption materials affect indoor air concentration as the building's pressurization fluctuates and how indoor air concentration are affected by indoor materials following successful mitigation of the structure.

2. Methods

2.1. Experimental Setup

The TCE dynamic sorption process of different building materials were determined by use of a method schematically shown in Figure 1. This method involved a selected material contained in an adsorption column through which TCE-containing gas was passed, and subsequent thermal desorption and measurement of the total amount of adsorption. During the adsorption part of the process, stainless steel tubes were packed with building materials held in place by glass wool. The amount of building material normally held in the tube was around 1 g. It was determined that neither the glass wool nor the stainless steel tube would retain significant amounts of TCE. The sample-containing tubes were first exposed desired low concentrations of TCE in nitrogen, which were then allowed to interact with the flow for varying periods of time. The typical flow rate of the nitrogen was 60 ml/min and the concentrations of TCE was around 1.1 ppbv. All of these adsorption experiments were conducted at room temperature. After a given time of exposure to the TCE-containing flow, that flow was stopped, and the sample tube was attached to a sorbent tube placed downstream of the sample tube. The sample tube was arranged such that the direction of the nitrogen flow in the subsequent desorption process was opposite that of the TCE-containing nitrogen flow during the adsorption process. During the thermal desorption step, the sample containing tube was covered by a heating mantle which permitted its heating at 100 °C. This allowed fully desorbing the TCE which had been held on the sample into a pure nitrogen flow, which carried it to the room temperature downstream sorbent tube, where it was again fully adsorbed. These tubes fully capture all of the TCE desorbed, from the sam-

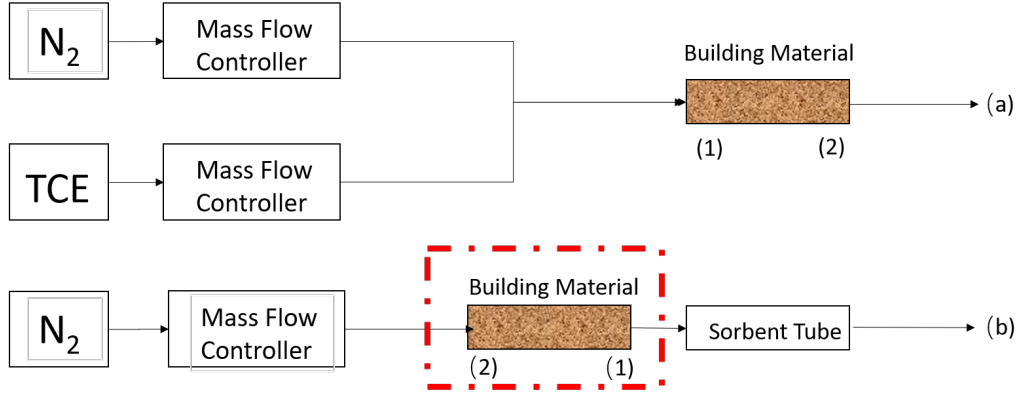


Figure 1: Schematic of experimental setup.

102 ples, and the amount of TCE was analyzed by Gas Chromatography (GC)
 103 with an Electron Capture Detector(ECD).

104 2.2. Numerical Model

105 To investigate the role of sorption in VI, we consider a simple VI scenario.
 106 Here we consider a house with a 10 by 10 m footprint, with the foundation
 107 bottom located 1 m below ground surface (bgs). The sole contaminant source
 108 is an uniformly TCE contaminated groundwater located 4 bgs, and the soil
 109 surrounding the house is assumed to homogenous and of a singular type. All
 110 contaminant vapors are assumed to enter the house through breaches in the
 111 foundation, modeled as a 1 cm wide crack that runs along the perimeter of
 112 the house. Finally we assume that sorption processes can occur both in the
 113 soil matrix and in the indoor environment (on various indoor materials).

114 Modeling this scenario requires us to simulate a couple of physics, many
 115 of which depend and interact with each other. The governing equations and
 116 the physics they govern are:

- 117 1. van Genuchten retention model - soil moisture.
- 118 2. Darcy's Law - air flow in the porous media.
- 119 3. Transport equation - contaminant transport in porous media.
- 120 4. Continuously stirred tank reactor (CSTR) - contaminant concentration
 121 in the indoor environment.

122 These physics are implemented in COMSOL Multiphysics, a commercial
 123 finite-element method package, which is used to solve our model. It is impor-

Figure 2: The vapor intrusion model

124 tant to note that the indoor environment is implicitly modeled, but instead
 125 only given by the CSTR equation; the soil domain is explicitly modeled.

126 2.2.1. Vadose Zone Moisture Content

127 Since the contaminant transport occurs through three-phased the vadose
 128 zone, it is important that we correctly account for soil moisture content and
 129 its effect on advective and diffusive transport. In this modeled scenario, we
 130 assume that the soil moisture is at steady-state and does not change, and
 131 thus the soil moisture content is given by the retention model developed by
 132 van Genuchten.

The van Genuchten retention model gives the soil water saturation as a function of elevation above groundwater. In turn this gives the water and gas filled porosities, and the relative permeability of the soil matrix.

$$\text{Se} = \begin{cases} \frac{1}{(1+\alpha z^n)^m} & z < 0 \\ 1 & z \geq 0 \end{cases} \quad (1)$$

$$\theta_w = \begin{cases} \theta_r + \text{Se}(\theta_s - \theta_r) & z < 0 \\ \theta_s & z \geq 0 \end{cases} \quad (2)$$

$$k_r = \begin{cases} \text{Se}^l [1 - (1 - \text{Se}^{\frac{1}{m}})]^2 & z < 0 \\ 0 & z \geq 0 \end{cases} \quad (3)$$

133 Se is the saturation, and ranges from 0 to 1, which represent completely un-
 134 to fully saturated; z is the elevation above the groundwater in meters; θ_r ,
 135 θ_s , θ_w , and θ_g are the residual moisture content, saturated porosity (or just
 136 porosity), and water and air filled porosities respectively. All units are in
 137 volume of phase divided by the volume of soil; k_r is the relative permeability
 138 of water, which modifies the saturated permeability. This too ranges from 0
 139 to 1, indicating completely im- and permeable respectively. $1 - k_r$ gives the
 140 relative permeability of air.

141 2.2.2. Gas Flow In The Vadose Zone

142 The gas flow in the vadose zone is governed by a modified version of
 143 Darcy's Law. Originally, Darcy's Law was developed to describe flow in
 144 saturated porous media, but since we're interested in flow in unsaturated

media, modification is necessary. An effective permeability that depends on the relative permeability from van Genuchten is introduced to allow for correct flow profiles in unsaturated porous media.

The vapor flow governing equation is given by

$$\frac{\partial}{\partial t}(\rho\theta_s) + \nabla \cdot \rho \left(- \frac{(1 - k_r)\kappa}{\mu} \nabla p \right) = 0 \quad (4)$$

Here ρ is the fluid density; ∇ is the del operator; κ is the saturated permeability; μ is the fluid viscosity; and p is the fluid pressure. We assume that the contaminant vapors are so dilute that the gas flow properties can be taken to be those of air, and specifically at 20 °C and all the transport properties may be found in Table 1.

Boundary Conditions. To solve (4) we assign the atmosphere boundary (see Figure 2) to be at reference pressure and act as a gauge, i.e. zero pressure. The foundation crack boundary is assigned the indoor-outdoor pressure difference value. Remaining boundaries are no-flow boundary conditions.

$$\text{Atmosphere} \quad p = 0 \text{ (Pa)} \quad (5)$$

$$\text{Foundation crack} \quad p = p_{\text{in/out}} \text{ (Pa)} \quad (6)$$

$$\text{All other} \quad -\vec{n} \cdot \rho_{\text{air}} \vec{u} = 0 \text{ (kg/(m}^2 \cdot \text{s))} \quad (7)$$

Here \vec{n} and \vec{u} are the boundary normal and gas velocity vectors.

Initial Conditions. For steady-state problems, the initial conditions don't matter, but is simply zero for the entire domain. When solving transient, the initial conditions are given by the steady-state solution.

2.2.3. Mass Transport In The Vadose Zone

Contaminants in the vadose zone exist in three phases - gaseous, solved in water, and sorbed onto soil particles. While there are three distinct phases, the water and gas phases are related via Henry's Law (8).

$$c_g = K_H c_w \quad (8)$$

Where c_g and c_w are the gas and water phase concentrations respectively in mol/m³; K_H is the dimensionless Henry's Law constant.

164 In this work, we consider sorption between the soil and vapor phases, as
 165 a function of the water contaminant concentration, through linear sorption
 166 (9).

$$c_s = K_{\text{ads}} \rho_b c_g = K_{\text{ads}} \frac{\rho}{1 - \theta_t} K_H c_w \quad (9)$$

167 Here the c_s is the solid phase concentration in mol/kg; ρ_b is the bulk density
 168 of the soil kg/m³, which is given by the density ρ and the total soil porosity
 169 θ_t ; K_{ads} is the sorption isotherm in m³/kg. Using Henry's Law and the linear
 170 isotherm we can express the total contaminant concentration in terms of the
 171 water contaminant concentration.

172 Mass transport in the vadose zone is governed by diffusion and advection
 173 and is given by (10).

$$R \frac{\partial c}{\partial t} = \nabla \cdot [D_{\text{eff}} \nabla c] - K_H \vec{u} \cdot \nabla c \quad (10)$$

174 The first term in (10) gives the change in contaminant water concentration
 175 with respect to time, modified by the *retardation factor*, R , which is discussed
 176 below; The second is the effective diffusive flux which is modified by the
 177 effective diffusion coefficient D_{eff} which is also discussed below. The third is
 178 the advective flux where \vec{u} is the soil-gas velocity from Darcy's Law, which
 179 when multiplied with K_H gives the gas phase concentration advective flux.

180 *Contaminant entry into the building.* The contaminant enters the building
 181 through a combination of advection and diffusive fluxes and is given by (11).

$$j_{ck} = \begin{cases} u_{ck} c_g - \frac{D_{\text{air}}}{L_{\text{slab}}} (c_{in} - c_g) & u_{ck} \geq 0 \\ u_{ck} c_{in} - \frac{D_{\text{air}}}{L_{\text{slab}}} (c_{in} - c_g) & u_{ck} < 0 \end{cases} \quad (11)$$

182 Here the j_{ck} is the molar contaminant flux into the building in mol/(m² · s);
 183 D_{air} is the contaminant diffusion coefficient in pure air in m²/s; L_{slab} is the
 184 thickness of the foundation slab in m. The flux expression changes if there
 185 is a bulk flow into the building, i.e. $u_{ck} \geq 0$, or out of the building.

186 *Retardation factor.* As the contaminants are transported through the vadose
 187 zone, the partitioning between the various phases increases the contaminant
 188 residency time, retarding the transport of contaminants. This effect is rep-
 189 resented by R which is the retardation factor (12).

$$R = \theta_w + \theta_g K_H + \rho_b K_H K_{\text{ads}} \quad (12)$$

Here θ_w , θ_g are the water and gas filled soil porosities; K_{ads} is the solid-gas phase sorption isotherm in m^3/kg . The diffusive and advective transport retardation is proportional to the inverse of R .

$$D_{\text{retarded}} = \frac{D_{\text{eff}}}{R} \quad (13)$$

$$\vec{u}_{\text{retarded}} = \frac{\vec{u}}{R} \quad (14)$$

190 It should be noted that the soil-gas velocity, \vec{u} , is not retarded in of itself,
 191 but rather just the contaminant being transported through advection, giving
 192 a effective bulk velocity.

193 *Effective diffusivity.* The effective diffusivity in the vadose zone varies with
 194 the soil moisture content, from being close to that in water when fully sat-
 195 urated and vice versa. Millington-Quirk developed (15) which describes the
 196 effective diffusivity in variably saturated porous media.

$$D_{\text{eff}} = D_{\text{water}} \frac{\theta_w^{\frac{7}{3}}}{\theta_t^2} + \frac{D_{\text{air}}}{K_H} \frac{\theta_g^{\frac{7}{3}}}{\theta_t^2} \quad (15)$$

197 Where the porosity fractions are the water and gas phase tortuosity terms;
 198 D_{air} and D_{water} are the contaminant diffusion coefficient in air and water
 199 respectively in m^2/s .

Boundary Conditions. A few boundary conditions are required to solve (10). In this model, the sole contaminant source is assumed to be the homogenously contaminated groundwater, which we assume to have a fixed concentration. The atmosphere acts as a contaminant sink, and any contaminant that makes it to this boundary is infinitely diluted, thus this is simply a zero concentration boundary condition. Contaminants leave the soil domain and enter the building through a combination of advective and diffusive gas phase transport. The last boundary condition is applied to all other boundaries and is a no-flow boundary.

$$\text{Groundwater} \quad c_w = 0 \text{ (mol/m}^3\text{)} \quad (16)$$

$$\text{Atmosphere} \quad c_w = c_{gw} \text{ (mol/m}^3\text{)} \quad (17)$$

$$\text{Foundation crack} \quad -\vec{n} \cdot \vec{N} = -\frac{j_{ck}}{K_H} \text{ (mol/(m}^2 \cdot \text{s))} \quad (18)$$

$$\text{All other} \quad -\vec{n} \cdot \vec{N} = 0 \text{ (mol/(m}^2 \cdot \text{s))} \quad (19)$$

200 $\vec{n} \cdot \vec{N}$ is the dot product between the boundary normal vector and the contam-
 201 inant flux; j_{ck} is the contaminant vapor flux into the building. We assume
 202 that only contaminants in the gas phase enter the building, and dividing j_{ck}
 203 by K_H we get proper accounting in terms of the water phase concentration.

204 *Initial Conditions.* For a steady-state condition the initial conditions don't
 205 matter, but are set to be zero everywhere. For transient simulations in this
 206 work, the steady-state solution is always used as an initial condition.

207 2.2.4. Indoor Environment

208 The indoor air space is modeled as a continuously stirred tank reactor
 209 (CSTR) given by (20). Contaminants are assumed to only enter through the
 210 foundation crack, represented by n_{ck} , which is calculated by integrating the
 211 contaminant flux over the foundation crack boundary. The product of air
 212 exchange rate, which govern how many house volumes are exchanged with
 213 the outside per time unit, and indoor air contaminant concentration gives the
 214 contaminant exit rate. The sorption of contaminant is given by the sorption
 215 reaction term in (22) and the sorbed contaminant concentration is given by
 216 (21).

$$V_{\text{bldg}} \frac{\partial c_{\text{in}}}{\partial t} = n_{\text{ck}} - A_e c_{\text{in}} V_{\text{bldg}} + r_{\text{sorb}} V_{\text{mat}} \quad (20)$$

$$V_{\text{mat}} \frac{\partial c_{\text{sorb}}}{\partial t} = -r_{\text{sorb}} V_{\text{mat}} \quad (21)$$

$$r_{\text{sorb}} = k_1 c_{\text{sorb}} - k_2 c_{\text{in}} \quad (22)$$

$$n_{\text{ck}} = \int_{A_{ck}} j_{ck} dA \quad (23)$$

217 Here V_{bldg} and V_{mat} are the indoor control volume and volume of indoor
 218 material in m^3 ; c_{in} and c_{sorb} are the indoor and sorbed (onto the indoor
 219 material) contaminant concentrations in mol/m^3 ; n_{entry} is the contaminant
 220 entry rate in mol/s , which is calculated by integrating the contaminant flux
 221 j_{ck} over the foundation crack area; r_{sorb} sorption rate in $\text{mol}/(\text{m}^3 \cdot \text{s})$; k_1 and
 222 k_2 are desorption and sorption reaction constants in $1/\text{s}$.

223 *Fitting Kinetic Parameters.* To calculate the indoor sorption rate we need k_1
 224 and k_2 . These values are found by solving (22) numerically and then finding
 225 the best k_1 and k_2 by fitting them to the experimental data via least square.

Table 1: Transport properties and model parameters

We use Runge-Kutta method of order 5(4) as the numerical solve, which is implemented together with the least square method in the SciPy python package[10].

3. Results & Discussion

3.1. Fitting Sorption Parameters

Using the numerical fitting scheme described in section 2.2.4 with the sorption data from the method described in section 2.1, the kinetic sorption parameters k_1 and k_2 are fitted. Figure 3 shows the result of this fitting and the sorption data for three select materials - wood, Appling soil, and cinderblock concrete. The k_1 and k_2 represent the rate at which TCE desorbs and sorbs respectively onto/from the material of interest. The equilibrium sorption constant is, using the formulation in (22), given by

$$K = \frac{k_1}{k_2} \quad (24)$$

and is used as the sorption isotherm. Here a small K indicate that there is a greater propensity for contaminant sorption.

To use the soil sorption isotherm in (10) K needs to be converted from being unitless to m^3/kg . This is done by multiplying the inverse of K isotherm with inverse of the soil bulk density ρ_b , which is taken to be $1460 \text{ kg}/\text{m}^3$.

$$K_{\text{ads}} = \frac{1}{K\rho_b} = 5.28 \text{ (m}^3/\text{kg)} \quad (25)$$

Table 2 shows the fitted parameters for the tested materials. Based on this these results we can see that cinderblock and soil have orders of magnitude larger sorption capacities than wood or drywall does. We can also see by the k_2 values that soil and cinderblock sorb quickly, much faster than a material with similar sorptive capacity such as paper.

3.2. Soil Sorption's Retarding Effect

Building pressurization is a key factor in VI that influences the advective contaminant transport. The magnitude of change in response to a pressurization change is significantly influenced by a range of factors, such as soil

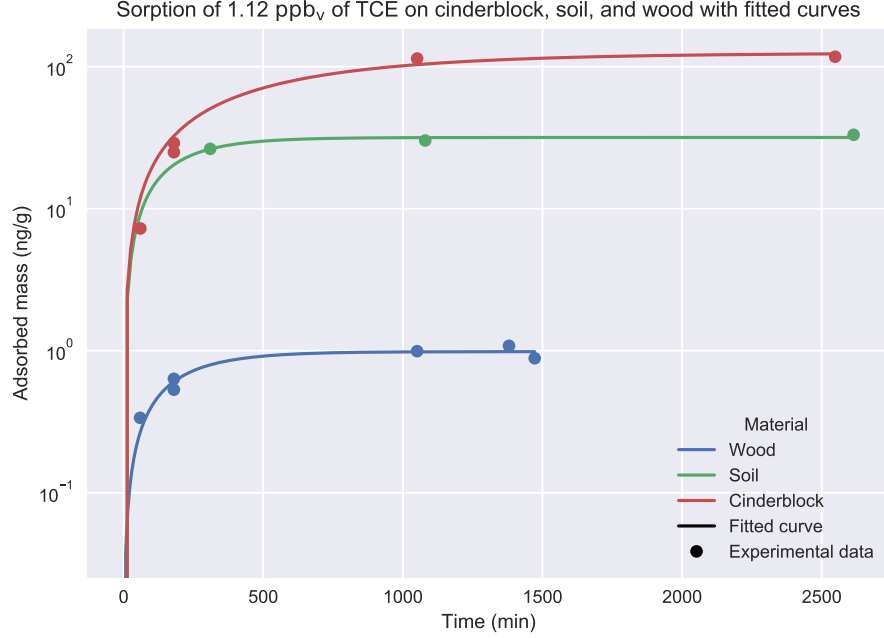


Figure 3: Experimental data of sorption of TCE onto three select materials as well as fitted sorption rates based on the kinetic model (22).

Table 2: Fitted kinetic sorption parameters based on sorption experiment data.

Material	k_1 (1/hr)	k_2 (1/hr)	K
Wood	0.32	44.90	$7.10 \cdot 10^{-3}$
Drywall	0.41	87.94	$4.65 \cdot 10^{-3}$
Carpet	0.26	58.74	$4.42 \cdot 10^{-3}$
Paper	0.04	88.37	$4.55 \cdot 10^{-4}$
Soil	0.34	2636.57	$1.30 \cdot 10^{-4}$
Cinderblock	0.10	4175.16	$2.40 \cdot 10^{-5}$

permeability, foundation depth, or soil moisture. To demonstrate the effect that soil sorption has on contaminant soil mass transport in the VI context, we run two types transient simulation where initially the modeled structure is at a steady -5 Pa, i.e. slightly depressurized. At the start of the simulation, the building building is 1) further depressurized to -15 Pa, or 2)

overpressurized to 15 Pa, and the simulation is allowed to run for 72 hours.

$$\text{Depressurization : } \Delta p_{\text{in/out}} = \begin{cases} -5, & t = 0 \text{ (hr)} \\ -15, & 0 < t \leq 72 \text{ (hr)} \end{cases} \quad (26)$$

$$\text{Overpressurization : } \Delta p_{\text{in/out}} = \begin{cases} -5, & t = 0 \text{ (hr)} \\ 15, & 0 < t \leq 72 \text{ (hr)} \end{cases} \quad (27)$$

249 For each of these cases, the simulation is run using two different soil types
 250 - sand and sandy loam. Sand is assumed here to not sorb any TCE, while
 251 for sandy loam a range of sorption isotherms are used. These range from
 252 no sorption ($K_{\text{ads}} = 0 \text{ (m}^3/\text{kg)}$) to the experimentally determined sorption
 253 isotherm ($K_{\text{ads}} = 5.28 \text{ (m}^3/\text{kg)}$).

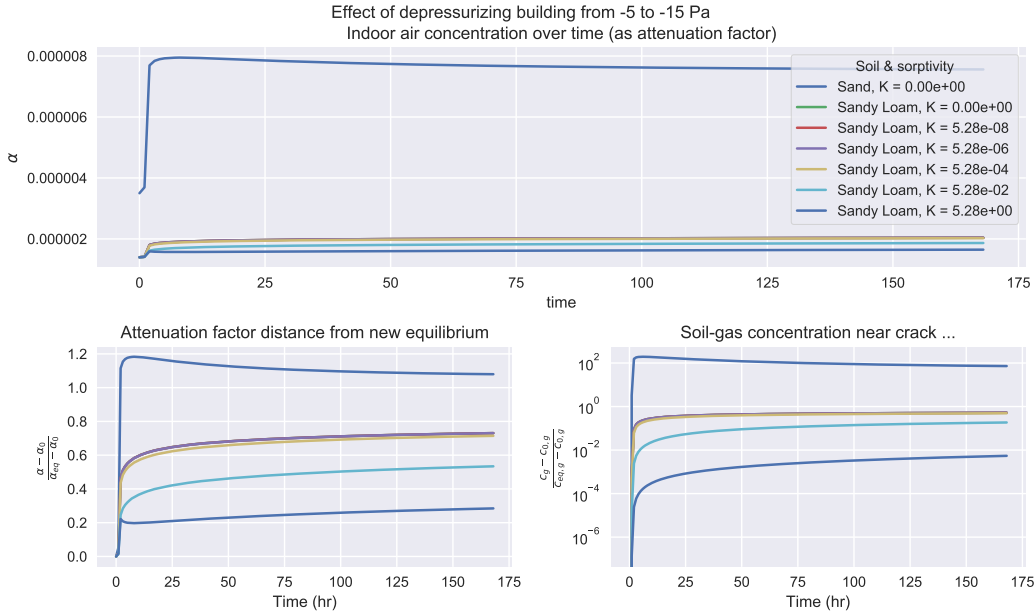


Figure 4

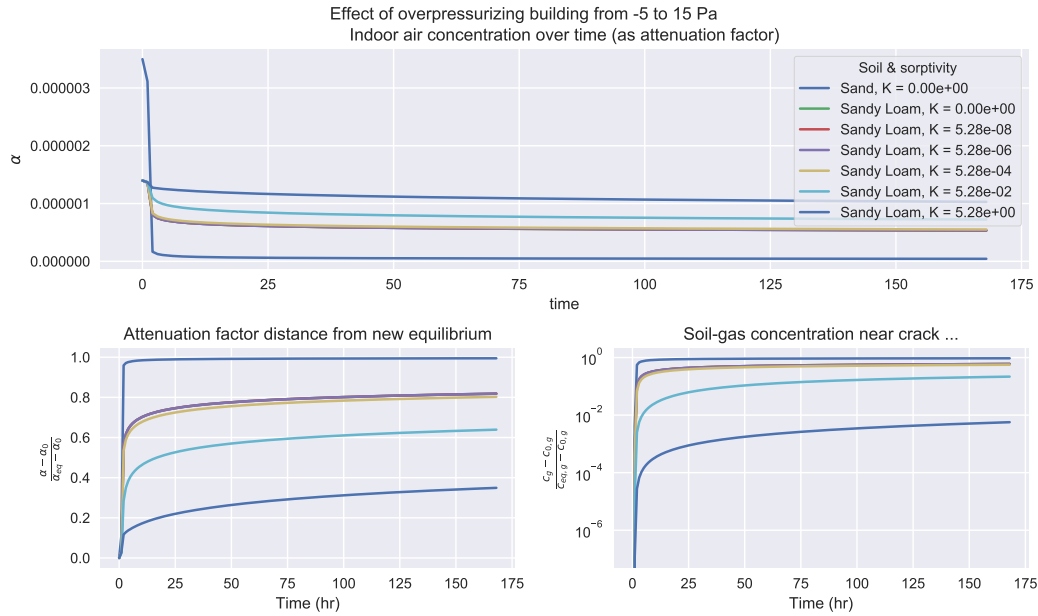


Figure 5

254 3.3. Indoor Material Sorption And Dynamics

255 3.4. Indoor Material Sorption And Mitigation

256 4. Conclusions

257 Acknowledgements

258 This project was supported by grant ES-201502 from the Strategic Envi-
259 ronmental Research and Development Program and Environmental Security
260 Technology Certification Program (SERDP-ESTCP).

261 Declaration of interest: none

262 References

263 [1] R. Meininghaus, L. Gunnarsen, H. N. Knudsen, Diffusion and Sorp-
264 tion of Volatile Organic Compounds in Building Materials-Impact on
265 Indoor Air Quality, Environ. Sci. Technol. 34 (15) (2000) 3101–3108.
266 doi:10.1021/es991291i.

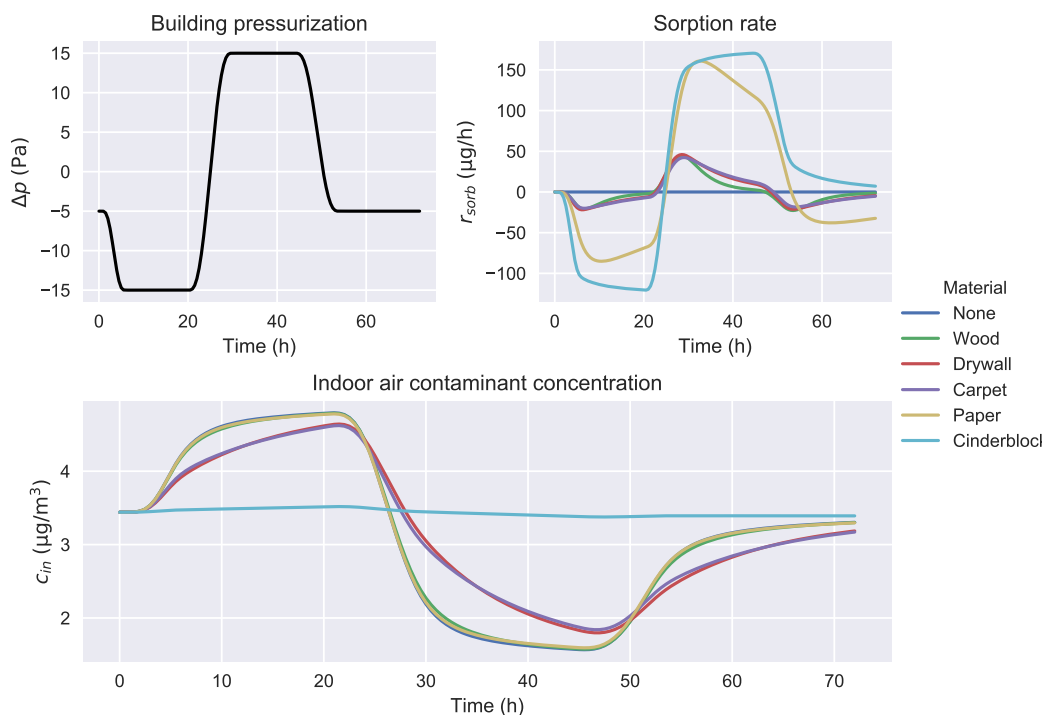


Figure 6

- [2] R. Meininghaus, E. Uhde, Diffusion studies of VOC mixtures in a building material, *Indoor Air* 12 (4) (2002) 215–222. doi:10.1034/j.1600-0668.2002.01131.x.
- [3] U.S. Environmental Protection Agency, OSWER Technical Guide for Assessing and Mitigating the Vapor Intrusion Pathway From Subsurface Vapor Sources To Indoor Air (2015).
- [4] C. Holton, Y. Guo, H. Luo, P. Dahlen, K. Gorder, E. Dettenmaier, P. C. Johnson, Long-Term Evaluation of the Controlled Pressure Method for Assessment of the Vapor Intrusion Pathway, *Environ. Sci. Technol.* 49 (4) (2015) 2091–2098. doi:10/f64j45.
- [5] C. C. Lutes, R. S. Truesdale, B. W. Cosky, J. H. Zimmerman, B. A. Schumacher, Comparing Vapor Intrusion Mitigation System Performance for VOCs and Radon, *Remediation* 25 (4) (2015) 7–26. doi:10/gd6dfn.

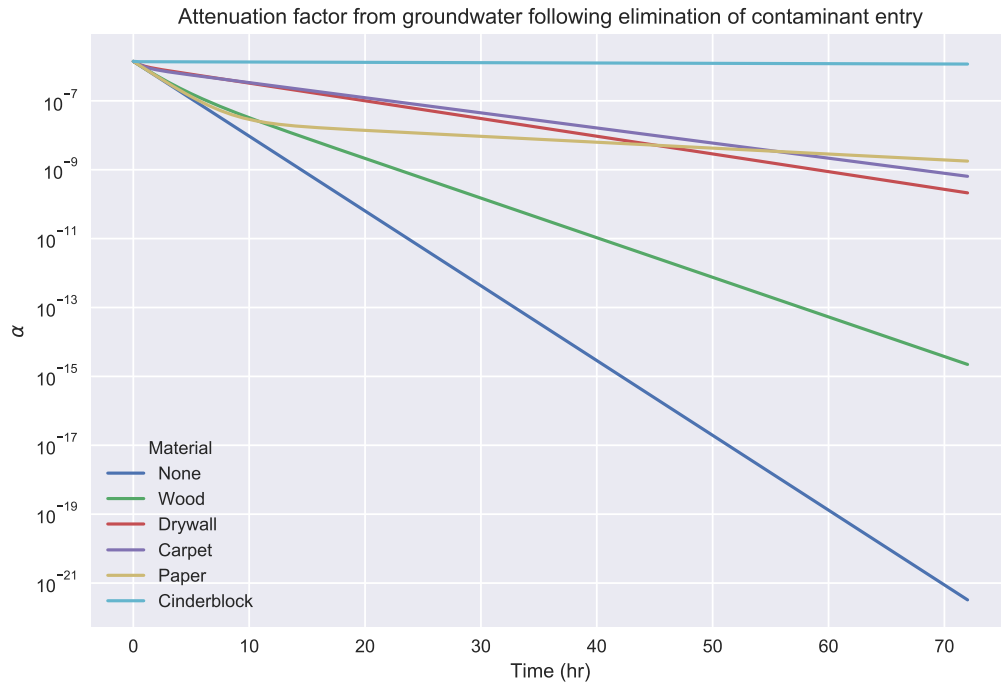


Figure 7

- 281 [6] U.S. Environmental Protection Agency, Assessment of Mitigation Sys-
 282 tems on Vapor Intrusion: Temporal Trends, Attenuation Factors, and
 283 Contaminant Migration Routes under Mitigated And Non-mitigated
 284 Conditions (2015).
- 285 [7] T. McHugh, P. Loll, B. Eklund, Recent advances in vapor intrusion
 286 site investigations, *Journal of Environmental Management* 204 (2017)
 287 783–792. doi:10/gd6dgk.
- 288 [8] R. Shen, K. G. Pennell, E. M. Suuberg, A numerical investigation of
 289 vapor intrusion — The dynamic response of contaminant vapors to
 290 rainfall events, *Science of The Total Environment* 437 (2012) 110–120.
 291 doi:10/f4fp9s.
- 292 [9] J. G. V. Ström, Y. Guo, Y. Yao, E. M. Suuberg, Factors affect-
 293 ing temporal variations in vapor intrusion-induced indoor air contam-

- 294 inant concentrations, Building and Environment 161 (2019) 106196.
295 doi:10.1016/j.buildenv.2019.106196.
- 296 [10] E. Jones, T. Oliphant, Pearu Peterson, SciPy: Open source scientific
297 tools for Python (2011).